Metal–organic framework nanofibers *via* electrospinning†‡

Rainer Ostermann,[a] Janosch Cravillon,[b] Christoph Weidmann,[a] Michael Wiebcke[b] and Bernd M. Smarsly*[a]

A hierarchical system of highly porous nanofibers has been prepared by electrospinning MOF (metal–organic framework) nanoparticles with suitable carrier polymers. Nitrogen adsorption proved the MOF nanoparticles to be fully accessible inside the polymeric fibers.

The design of hierarchical nanostructures is a long-sought goal of materials science and there has been extensive research into various "top-down" and "bottom-up" methods to create these nanostructures. Electrospinning is one of the simplest top-down methods that allows for an easy generation of nanofibers from a wide variety of materials, especially polymers which were proven to be useful for many applications like filtration or controlled drug-release.[1,2]

However, in spite of various attempts, the preparation of porous polymeric nanofibers with high surface areas could not be realized so far.

Isotactic polymers like PLLA (poly-L-lactide) and blends thereof[3,4] have been electrospun from solvent mixtures to produce porous fibers.[5] Another approach applicable to various polymers is to use a cryogenic liquid to trap some of the solvent inside the fibers, followed by an extraction of the solvent under reduced pressure to yield some porosity.[6] However, the specific surface area of such "porous" polymeric fibers is always quite low, usually in the range of 10–15 $m^2\,g^{-1}$, corresponding only to an increase by a factor of 2–3 compared to the corresponding "non-porous" fibers. Only in inorganic or carbonized PAN (polyacrylonitrile) fibers sufficient microporosity can be found allowing for surface areas of up to 300 or 600 $m^2\,g^{-1}$ respectively.[7,8] Highly porous polymers remain special cases with a high degree of (hyper)cross-linking like PIMs (polymers of intrinsic porosity)[9–11] and have not been prepared in the form of nanofibers so far.

In contrast, metal–organic frameworks (MOF) are crystalline coordination polymers that are well known for their extremely high porosity and surface areas.[12] Zeolitic imidazolate framework (ZIF) materials constitute a new subclass of MOFs that combine the properties of porous MOFs with high chemical and thermal stability.[13] Various MOFs, including ZIFs, have been very recently used as fillers for the fabrication of mixed matrix membranes.[14,15]

In order to achieve a homogeneous distribution of filler particles within an organic polymer matrix it should be beneficial to use monodisperse nanoparticles. Recently, Cravillon *et al.* succeeded in preparing nanocrystals of a prototypical ZIF material, ZIF-8, that are 50 nm in size and have a rather narrow size distribution.[16]

Similar nanocrystals have recently been shown to exhibit distinct advantages like faster adsorption kinetics for porous coordination polymers.[17]

In this work we present for the first time the synthesis and characterization of composite MOF–polymer nanofibers combining the advantages of both types of materials to achieve a novel class of hierarchical nanostructure.

The colloidal suspensions of ZIF-8 nanoparticles in methanol were prepared as described before.[16] Briefly, a solution of appropriate amounts of $Zn(NO_3)_2 \cdot 6H_2O$ and 2-methylimidazole in methanol was stirred at room temperature for 1 h, before separating the resulting nanocrystals by centrifugation. The ZIF-8 nanoparticles were redispersed in fresh methanol by vortex mixing and ultrasonic agitation and a part of the solution was dried at 80 °C under reduced pressure to determine the concentration to be 3.5–4.5 wt% of ZIF-8. In a typical electrospinning experiment, 500 mg of a solution of 12 wt% PVP (polyvinylpyrrolidone, molecular weight (MW) = 1 300 000) in methanol was added to 400–2000 mg of the ZIF-8 dispersion and mixed thoroughly. The solution was diluted or concentrated under reduced pressure to yield a final concentration of 3.5 wt% of PVP. This solution was fed through a metallic needle by a syringe pump (KDS scientific) at the rate of 0.35 ml h^{-1}. The needle is placed at a distance of 6–8 cm from the aluminium foil that serves as collector and a voltage of 5 kV (Spellman CZE1000R high-voltage power supply) was applied to produce a non-woven mat (see Fig. 1–3). The composite PVP–ZIF-8 nanofibers and the dried ZIF nanoparticles were characterized by SEM (LEO Gemini 982), TEM (Philips CM30-ST), XRD (Panalytical X'Pert PRO diffractometer) and N_2 adsorption (Quantachrome Autosorb 1 and 6).

The diameter of the nanofibers could be adjusted by the polymer concentration and was found to be roughly 150–300 nm. The nanoparticle loading could be as high as 1 : 1 by weight ratio of ZIF-8 to PVP. SEM and TEM revealed a homogeneous distribution of the nanoparticles inside the fibers with a smooth polymeric surface.

As can be seen from Fig. 3, macroscopic non-wovens can be obtained on the centimetre scale. Thus, the composite fibers can be regarded as a "MOF textile", combining the properties of polymeric fibers and MOFs.

[a] *Institute of Physical Chemistry, Justus-Liebig-University Giessen, 35392 Giessen, Germany.*
E-mail: bernd.smarsly@phys.chemie.uni-giessen.de;
Fax: +49 641 9934509; Tel: +49 641 9934590
[b] *Institute of Inorganic Chemistry, Leibniz University Hannover, Callinstrasse 9, D-30167 Hannover, Germany*

† This article is part of the 'Emerging Investigators' themed issue for ChemComm.
‡ Electronic supplementary information (ESI) available: XRD data; SEM images; adsorption kinetics; description of fiber generation. See DOI: 10.1039/c0cc02271c
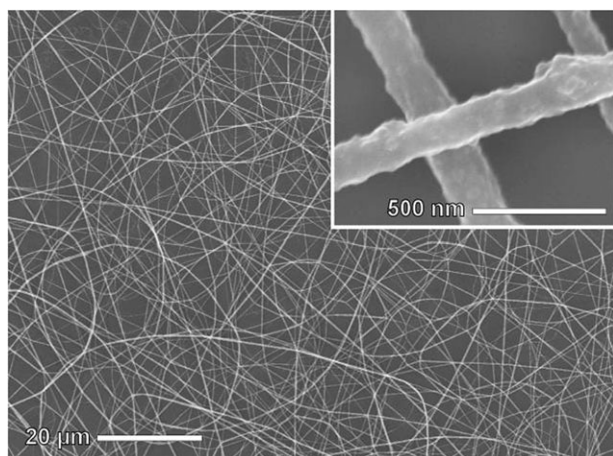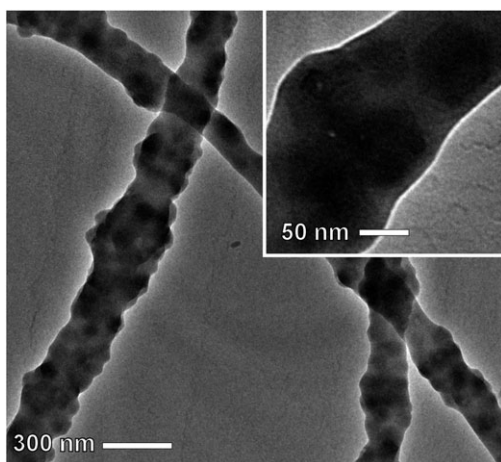
Fig. 1 SEM of ZIF-8 nanoparticles in PVP.

Fig. 2 TEM of ZIF-8 nanoparticles in PVP.

Fig. 3 Digital photograph of a non-woven ZIF-8–PVP fiber mat. The diameter is *ca.* 1.5 cm.

A comparison of XRD patterns of the ZIF-8 nanofibers and the pure nanoparticles showed the crystal structure to be preserved (see ESI‡). From N_2 adsorption measurements (Fig. 4) including micropore analysis, the surface area according to the BET model was 960 m^2 g^{-1} for the pure ZIF-8, while the
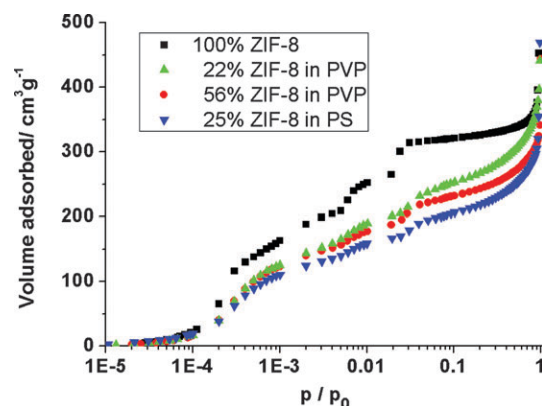

Fig. 4 Nitrogen adsorption isotherms of ZIF-8 nanoparticles in PS and PVP (with different loadings of ZIF-8). For clarity the desorption branch is omitted and the curves have been scaled to 100% ZIF-8 content.

Table 1 Nitrogen adsorption data

Sample	ZIF-8 concentration[a] (wt%)	Micropore volume/ cm^3 g^{-1}	Surface area[b]/ m^2 g^{-1}	Accessible ZIF-8 fraction[b] (wt%)
ZIF-8	100	0.49	960	100
ZIF in PVP	56	0.18	530	55.1
ZIF in PVP	22	0.07	180	19.1
ZIF in PS	25	0.07	210	22.7
PVP only	0	<0.002	10	n/a

[a] As weighed in. [b] According to the BET model.

fibers possessed surface areas of up to 530 m^2 g^{-1} for a weight ratio of approx. 1 : 1 ZIF-8 to PVP. As can be seen in Fig. 4, the adsorption branch for the fibers is shifted to higher pressure. The two steps on the adsorption isotherms that have been ascribed[18] to pressure-induced adsorbate reorganization are less pronounced, but still visible for the composite fibers. For lower loadings of ZIF-8 (see Table 1) the surface area decreased accordingly, proving the ZIF-8 nanoparticles to be fully accessible inside the polymeric nanofibers.

The nanofibers are stable in the as-prepared form up to 150 °C and do not degrade in organic solvents such as hexane, but are sensitive to polar solvents of the polymer such as alcohol or water, causing the nanofibers to coalesce.

Using other polymers like polystyrene (PS) and polyethylene oxide (PEO) allows increasing the fibers' stability and widening the range of possible applications.

In particular, the PS-ZIF-8 nanofibers are stable in alcohols and water and the surface area was fully accessible (determined by nitrogen sorption), even if the ZIF-8 loading up to 25 wt% was slightly lower. Higher loadings should be possible by tuning the synthesis parameter and functionalizing the surface of the ZIF-8 nanoparticles with less polar molecules (see ESI‡ for details of preparation).

The adsorption measurements show that the ZIF-8 nanoparticles are fully accessible. We further compared the adsorption kinetics of the nanofibers to bare nano- and micrometer-size particles (prepared by classical solvothermal synthesis and
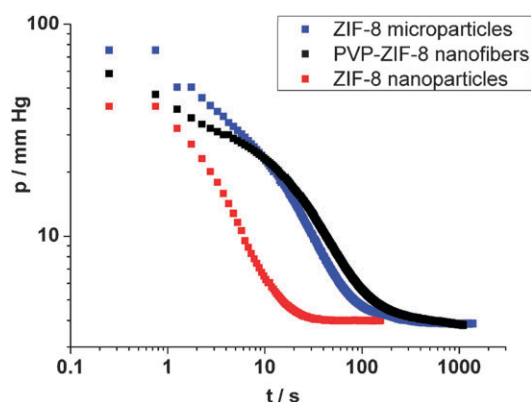
Fig. 5 N_2 adsorption kinetics studied as cell pressure over time.

referred to as "microparticles") by determining the time to reach equilibrium pressure after dosing a defined amount of adsorbate into the evacuated sample cell.

Although we cannot propose a model yet, it is obvious that diffusion inside the ZIF-8 is much slower than in the gas phase and that external surface area and the presence of a polymer layer determine the kinetics of adsorption.

As can be seen in Fig. 5 the nanoparticles attain equilibrium after 30 s, while the microparticles and the nanofibers require 100–120 s.

Most of the faster kinetics of the nanoparticles can probably be accounted for by the larger external surface area being ten times larger compared to the microparticles, while diffusion inside ZIF-8 is fast. The polymer layer around the fibers constitutes an additional diffusion barrier, therefore the nitrogen uptake is also slower than for the pure nanoparticles, but still as fast as for the microparticles. In fact, a low thickness of the polymer layer is crucial, as for polymer films or coalesced fiber mats, the kinetics become too slow to observe significant adsorption and accessible surface areas drop below 20 m² g⁻¹.

The results from N_2 adsorption were corroborated by CO_2 as adsorbate (see ESI‡ for isotherms and kinetics data).

Further results indicate that the different carrier polymers also affect the adsorption kinetics. It is found that the uptake is faster for PVP than for PS- and PEO-based nanofibers (see ESI‡ for SEM pictures, N_2 isotherms and kinetics data). In this regard, blends of polymers hold great promise as well.

As the carrier polymers and the degree of nanoparticle coverage by the polymer should also influence the absorption, this might allow tuning the selectivity of adsorption, especially with different gases. Therefore we are planning a systematic study for more relevant adsorbates like hydrogen, carbon dioxide or monoxide. Due to their low resistance to fluid flow, the nanofiber mats could ultimately be useful to selectively adsorb specific gases, for example carbon monoxide in gas masks.

In conclusion, we could prepare nanofibers of a metal–organic framework for the first time by electrospinning preformed nanoparticles, thereby creating hierarchical nanofibers with high surface areas and good accessibility. With the anticipated availability of other MOF materials as nanoparticles, a broad variety of MOF nanofibers should be accessible with various applications, for example in gas adsorption and separation.

Notes and references

1 D. Li and Y. Xia, *Adv. Mater.*, 2004, **16**, 1151–1170.
2 A. Greiner and J. Wendorff, *Angew. Chem., Int. Ed.*, 2007, **46**, 5670–5703.
3 M. Bognitzki, W. Czado, T. Frese, A. Schaper, M. Hellwig, M. Steinhart, A. Greiner and J. H. Wendorff, *Adv. Mater.*, 2001, **13**, 70–72.
4 M. Bognitzki, T. Frese, M. Steinhart, A. Greiner, J. H. Wendorff, A. Schaper and M. Hellwig, *Polym. Eng. Sci.*, 2001, **41**, 982–989.
5 Z. Qi, H. Yu, Y. Chen and M. Zhu, *Mater. Lett.*, 2009, **63**, 415–418.
6 J. T. McCann, M. Marquez and Y. Xia, *J. Am. Chem. Soc.*, 2006, **128**, 1436–1437.
7 M. Kanehata, B. Ding and S. Shiratori, *Nanotechnology*, 2007, **18**, 315602.
8 Z. Zhang, X. Li, C. Wang, S. Fu, Y. Liu and C. Shao, *Macromol. Mater. Eng.*, 2009, **294**, 673–678.
9 N. B. McKeown, S. Hanif, K. Msayib, C. E. Tattershall and P. M. Budd, *Chem. Commun.*, 2002, 2782–2783.
10 P. M. Budd, E. Elabas, B. Ghanem, S. Makhseed, N. McKeown, K. Msayib, C. Tattershall and D. Wang, *Adv. Mater.*, 2004, **16**, 456–459.
11 N. B. McKeown, B. Gahnem, K. J. Msayib, P. M. Budd, C. E. Tattershall, K. Mahmood, S. Tan, D. Book, H. W. Langmi and A. Walton, *Angew. Chem., Int. Ed.*, 2006, **45**, 1804–1807.
12 G. Ferey, *Chem. Soc. Rev.*, 2008, **37**, 191–214.
13 A. Phan, C. J. Doonan, F. J. Uribe-Romo, C. B. Knobler, M. O'Keeffe and O. M. Yaghi, *Acc. Chem. Res.*, 2010, **43**, 58–67.
14 K. Díaz, L. Garrido, M. López-González, L. F. del Castillo and E. Riande, *Macromolecules*, 2010, **43**, 316–325.
15 S. Basu, M. Maes, A. Cano-Odena, L. Alaerts, D. E. De Vos and I. F. Vankelecom, *J. Membr. Sci.*, 2009, **344**, 190–198.
16 J. Cravillon, S. Muenzer, S. Lohmeier, A. Feldhoff, K. Huber and M. Wiebcke, *Chem. Mater.*, 2009, **21**, 1410–1412.
17 D. Tanaka, A. Henke, K. Albrecht, M. Moeller, K. Nakagawa, S. Kitagawa and J. Groll, *Nat. Chem.*, 2010, **2**, 410–416.
18 K. S. Park, Z. Ni, A. P. Côté, J. Y. Choi, R. Huang, F. J. Uribe-Romo, H. K. Chae, M. O'Keeffe and O. M. Yaghi, *Proc. Natl. Acad. Sci. U. S. A.*, 2006, **103**, 10186–10191.